



TiO₂ mediated photocatalytic oxidation of volatile organic compounds: Formation of CO as a harmful by-product

D.S. Selishchev^{a,b,c,*}, N.S. Kolobov^{a,b,c}, A.A. Pershin^d, D.V. Kozlov^{a,b,c}

^a Boreskov Institute of Catalysis, Novosibirsk, 630090, Russian Federation

^b Novosibirsk State University, Novosibirsk, 630090, Russian Federation

^c Research and Educational Center for Energy Efficient Catalysis in Novosibirsk State University, Novosibirsk, 630090, Russian Federation

^d AIRLIFE LLC, Moscow, 119334, Russian Federation



ARTICLE INFO

Article history:

Received 12 April 2016

Received in revised form 21 July 2016

Accepted 25 July 2016

Available online 26 July 2016

Keywords:

Photocatalytic oxidation

TiO₂

VOCs

CO formation

Selectivity

ABSTRACT

Photocatalytic oxidation (PCO) of volatile organic compounds (VOCs) including acetone, alcohols and hydrocarbons was investigated in a static reactor using an FTIR *in situ* method. Three commercially available TiO₂ powders and one TiO₂ sample synthesized via thermal hydrolysis of titanyl sulfate were employed in the kinetic experiments. PCO reactions were conducted under different UV light intensities, initial concentrations of substrates, humidities, and temperatures. The formation of the final oxidation products and the kinetics of their accumulation were investigated.

Analysis of the FTIR spectra revealed the formation of CO along with CO₂ and H₂O as final products in the oxidation of VOCs over all the TiO₂ samples. No other final products were detected. The method of spectral subtraction by minimizing the IR spectrum length was applied to accurately calculate the CO concentration. The conversion of organic substrates to CO did not exceed 5%. The differential selectivity of CO₂ formation towards CO formation, which was defined as the initial CO₂ rate divided by the sum of the initial CO₂ and CO rates, was used to investigate the effect of the experimental parameters and the photocatalyst on the product distribution. The experimental conditions including light intensity, initial concentration and humidity as well as the photocatalyst and its pretreatment method did not exhibit a significant effect on the differential CO₂ selectivity during acetone oxidation but an increase in the reaction temperature resulted in a decrease in the CO₂ selectivity. A stronger influence was observed for the type of oxidizing substrate. The increase in the number of carbon atoms in the homologous series of C₂–C₄ alcohols and C₆–C₁₀ alkanes slightly decreased the CO₂ selectivity. The most substantial effect was related to the extent of unsaturation in the C₆ hydrocarbons. The CO₂ selectivity decreased from 98.9% for hexane to 93.3% for benzene. Benzene exhibited the highest conversion to CO (approximately 5%) among all the studied substrates.

Only the deposition of Pt (1 wt.%) completely prevented the formation of CO during the photocatalytic oxidation of VOCs both at low and high UV intensity.

Finally, the mechanism of CO formation is discussed.

© 2016 Elsevier B.V. All rights reserved.

1. Introduction

Currently, environmental pollution that is primarily caused by hazardous emissions from industry, energy production and motor transport is a worldwide challenge. Along with CO, SO₂ and NO_x, a significant part of pollutants are VOCs [1].

New technologies to protect the environment are currently being developed. Photocatalytic oxidation processes using TiO₂-based photocatalysts are regarded as one of the promising methods for controlling air pollution due to VOCs.

TiO₂ is a semiconductor material with an energy band gap of 3.0 and 3.2 eV for the rutile and anatase crystal phases, respectively [2]. When TiO₂ absorbs UV light, electrons are excited from the valence band to the conduction band, resulting in valence band electron vacancies (i.e., holes) [3]. In addition to recombination, photogenerated electrons and holes can migrate to the surface of TiO₂ particles and participate in surface redox reactions. The main route for photogenerated electron conversion involves reactions with surface

* Corresponding author at: Boreskov Institute of Catalysis, Novosibirsk, 630090, Russian Federation.

E-mail address: selishev@catalysis.ru (D.S. Selishchev).

oxygen, which result in reactive oxidants, such as $O^{•-}$, $OOH^{•}$, H_2O_2 and $OH^{•}$, on the TiO_2 surface. These species are capable of oxidizing organic molecules adsorbed on TiO_2 . The main routes for photogenerated hole conversion include interactions with adsorbed water and surface hydroxyl groups, which result in the formation of $OH^{•}$, or direct interaction with adsorbed organic molecules, which results in their oxidation. The high redox potential of the photo-generated holes [4] and the formation of powerful oxidants (e.g., hydroxyl radicals) result in nearly all the organic compounds being completely oxidized to CO_2 and H_2O over irradiated TiO_2 .

The photocatalytic process occurs through the gradual oxidation of the initial substrate, resulting in the formation of organic intermediates on the TiO_2 surface. In some cases, these intermediates can desorb from the surface of the photocatalyst and be detected in the gas phase [5]. Wada et al. observed the formation of aldehydes and ketones during the photocatalytic oxidation of simple C_1 – C_3 alkanes [6]. A small amount of acetaldehyde was detected in the gas phase during the photocatalytic oxidation of hexane [7,8]. Acetaldehyde was also observed as a main gas-phase intermediate during ethanol vapor photooxidation [9–11]. Maira et al. observed a small amount of benzaldehyde during the gas-phase photooxidation of toluene using a nanosized TiO_2 photocatalyst.

The composition of the reaction products during the photocatalytic oxidation process depends on the irradiation time and type of oxidized substrate. Under long-term UV irradiation, the complete oxidation of all the gas-phase organic intermediates to final oxidation products (i.e., CO_2 and H_2O) can be achieved. For example, in a kinetic experiment in a static reactor, organic intermediates initially accumulate in the gas phase and then, these intermediates are completely removed. At the same time, the level of formed CO_2 permanently increases and reaches a constant value at the end of a long period of irradiation [12–14].

In addition to organic intermediates, CO can be formed in the gas phase during the photocatalytic oxidation of VOCs [15]. Our previous studies [16–18] revealed that CO is almost always as a final product along with CO_2 and H_2O for the photooxidation of acetone, cyclohexane and diethyl sulfide vapor. This result is due to the very low quantum efficiency of CO photocatalytic oxidation over pure TiO_2 , especially in the low concentration range [19]. The integral selectivity of CO_2 formation towards CO at the end of the reaction was approximately 96–99% and depended on the type of organic substrate.

Few studies have focused on the formation of CO as a by-product in the photocatalytic oxidation of VOCs [20–24] due to the complicated quantitative analysis of extremely low concentrations of CO. In addition, a noticeable accumulation of CO is typically observed in experiments with a relatively high substrate concentration.

Therefore, in this study we investigated several commercially available and synthesized TiO_2 photocatalysts for the oxidation of different types of VOCs with special attention to CO formation. The effects of the photocatalyst, UV light intensity, humidity, temperature, type of organic substrate and initial substrate concentration on the differential selectivity of CO_2 formation towards CO formation were investigated.

2. Experimental

2.1. Materials

The following chemical reagents were used as test organic substrates in the photocatalytic experiments: methanol (CH_3OH), ethanol (C_2H_5OH), propanol-1 (C_3H_7OH), acetone (CH_3COCH_3), butanol-1 (C_4H_9OH), *n*-hexane (C_6H_{14}), cyclohexane (C_6H_{12}), cyclohexene (C_6H_{10}), benzene (C_6H_6), *n*-heptane (C_7H_{16}), *n*-octane (C_8H_{18}), *n*-nonane (C_9H_{20}) and *n*-decane ($C_{10}H_{22}$). All the chemicals

were high purity grade and applied as purchased from AO REAHIM Inc. (Russia) without further purification.

Three commonly used commercially available TiO_2 powder photocatalysts, including TiO_2 Hombifine N (marked in the paper as HF) from Sachtleben Chemie GmbH (Germany), TiO_2 P25 (marked as P25) from Evonik Industries AG (Germany) and TiO_2 KRONOS vlp 7000 (marked as VLP7000) from KRONOS TITAN GmbH Inc. (Germany), were employed in the photocatalytic oxidation of the organic substrates.

In addition to the commercially available TiO_2 samples, one TiO_2 photocatalyst was synthesized via the thermal hydrolysis of a $TiOSO_4$ by boiling $TiOSO_4$ water solution according to a previously published procedure [17]. This sample is referred to as TiO_2 -s.

2.2. Photocatalyst pretreatments

The following pretreatment methods were employed to investigate the effect of the surface chemistry of TiO_2 on CO formation:

- (1) TiO_2 HF was treated with 4 M H_2SO_4 for 2 h at 60 °C. This sample is referred to as HF-SO₄.
- (2) TiO_2 HF was calcined at 550 °C for 5 h to investigate the effect of surface OH-groups on CO formation. This sample is referred to as HF-550.
- (3) TiO_2 HF was modified by deposition of Pt to increase the rate of CO removal during the photocatalytic oxidation of VOCs. The Pt/ TiO_2 photocatalysts were prepared via the chemical reduction of a Pt-containing precursor with $NaBH_4$. Typically, 2 g of TiO_2 HF was suspended in 30 mL of distilled water, and a certain aliquot of an aqueous solution of H_2PtCl_6 was added. To reduce the metal precursor, a three-fold excess of $NaBH_4$ was added to the solution. The estimated content of noble metal in the Pt/ TiO_2 sample was 1 or 0.02 wt.%. The samples are referred to as HF-1Pt and HF-0.02Pt, where the number corresponds to the estimated Pt content.

2.3. Characterization techniques

The textural properties of the photocatalysts were investigated by N_2 adsorption at 77 K using an ASAP 2400 instrument (Micromeritics, USA). The surface area was calculated by BET analysis, the average pore diameter was determined by analysis of the BJH pore distribution, and the pore volume was determined as the total pore volume at $P/P_0 \sim 1$.

The crystal phase composition was determined by powder X-ray diffraction using a D8 Advance diffractometer (Bruker AXS GmbH, Germany) with $CuK\alpha$ radiation and scanning in a 2θ range of 15–85°.

The noble metal content in the Pt/ TiO_2 samples was measured by X-ray fluorescence analysis on an ARL spectrometer (Thermo Scientific, USA) with rhodium anode. The content was determined to be 0.99 or 0.02 wt.%, respectively.

2.4. Kinetic experiments

Kinetic experiments were performed in a 0.3 L static reactor that was installed in the cell compartment of a Nicolet 380 FTIR spectrometer (Thermo Scientific, USA). The schematic diagram of the experimental setup is shown in Fig. 1. The details of the experimental setup were described in our previous study [16].

Typically, the sample was uniformly deposited onto a 9.1 cm² glass support to obtain a layer with a surface density of 2 mg/cm². The glass support with the sample was placed into the reactor and irradiated by a high performance UV LED (Nichia, Japan) at $\lambda_{max} \sim 373$ nm for 2 h to completely oxidize all the organic species previously adsorbed on the photocatalyst surface. The initial rela-

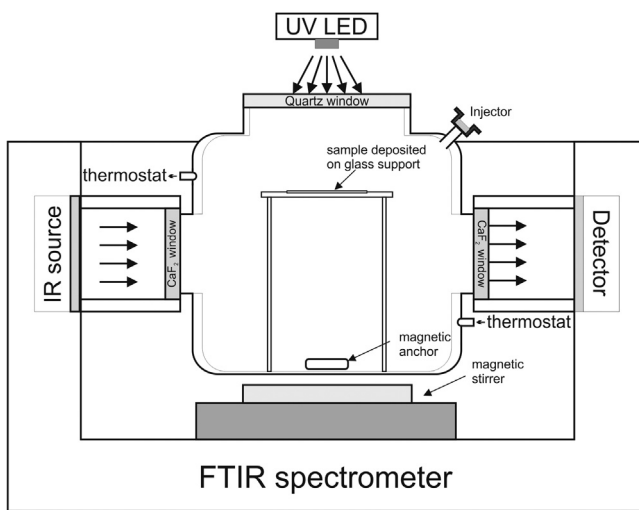


Fig. 1. Static reactor for the kinetic experiments: the reactor volume is 0.3 L, the optical path length is 10 cm.

tive humidity in the reactor was adjusted to 15 or 70% by initially flowing air with a specific humidity through the reactor.

Then, 1 or 2 μL of the organic substrate was injected into the reactor. After the 30 min time period that was required to achieve adsorption-desorption equilibrium, the UV LED was turned on again to initiate the photocatalytic oxidation. The irradiation continued until the amount of CO_2 accumulated in the reactor reached the expected level calculated from the stoichiometric equation.

To monitor the concentrations of the substrate and oxidation products in the reactor during the experiment, the IR spectra were collected periodically every 3 min. The quantitative analysis of the organic substrates and CO_2 was performed by the integration of collected IR spectra using the Beer-Lambert law as follows:

$$\int_{\omega_1}^{\omega_2} A(\omega) d\omega = \varepsilon \cdot I \cdot C$$

where $A(\omega) = \lg \left(\frac{I_0(\omega)}{I(\omega)} \right)$ is the absorbance, ω_1 and ω_2 are the limits of the corresponding absorption band (cm^{-1}), ε is the coefficient of extinction ($\text{ppm}^{-1} \text{cm}^{-2}$), I is the optical path length (cm), and C is the concentration of substance in the gas phase (ppm).

In contrast to the results for the organic substrates and CO_2 , the calculation of the CO concentration according to the Beer-Lambert law as described above led to very low accuracy. Therefore, the method of spectral subtraction, that is based on minimization of the length of the spectrum resulting from subtracting the calibration CO spectrum from the experimental spectrum of the gas mixture [25], was applied for analysis of this substance. The advantage of this method is the accurate calculation of low admixtures concentration (e.g., CO).

Based on the results of the analysis of the collected IR spectra, the kinetic curves for the substrate, CO_2 and CO in form of the concentration versus the time taken from the recording time of IR spectra were plotted. The initial rates of CO_2 ($W_{\text{CO}_2}^0$) and CO (W_{CO}^0) formation were focused on during the photooxidation of organic substrates. These values were calculated by the linearization of the initial part of the CO_2 and CO kinetic curves. Based on the CO_2 and CO rates, the differential selectivity (S_{CO_2}) of CO_2 formation towards CO formation can be expressed as follows:

$$S_{\text{CO}_2} = \frac{W_{\text{CO}_2}^0}{W_{\text{CO}_2}^0 + W_{\text{CO}}^0} \cdot 100\%$$

The differential selectivity was chosen because it is more accurate compared to the integral selectivity, which is defined as the final amount of CO_2 divided by the sum of the final amounts of CO and CO_2 , and allows us to take into account the influence of the activity of the photocatalyst.

The CO_2 selectivity was used for comparison of the different photocatalysts and different oxidizing substrates.

3. Results and discussion

3.1. Characteristics of the photocatalyst

All the studied photocatalysts have different textural properties.

The largest surface area was observed for the TiO_2 HF photocatalyst prepared by the sulfate technology from a natural mineral ilmenite (Table 1). The treatments of HF by sulfuric acid or noble metal deposition did not have a strong influence on its textural properties. In contrast, the calcination of HF at 550 °C substantially decreased the surface area (61 m²/g) and pore volume (0.27 cm³/g).

A large surface area (296 m²/g) and pore volume (0.41 cm³/g) were also observed for the TiO_2 VLP7000 photocatalyst. The TiO_2 P25 photocatalyst, which is a pyrogenic oxide, exhibited the smallest textural parameters among all the commercial photocatalysts (i.e., surface area of 81 m²/g and pore volume of 0.27 cm³/g).

In addition to the commercial photocatalysts, one more TiO_2 photocatalyst was prepared in the laboratory and tested. The TiO_2 -s sample was prepared via titanyl sulfate thermal hydrolysis. In contrast to the widely used sol-gel method, this method does not require a high temperature treatment and allows for the preparation of anatase TO_2 with high crystallinity and small crystallites. Therefore, the synthesized TiO_2 -s sample had a large surface area of 222 m²/g.

According to the official technical documentation, the TiO_2 HF was composed of 100% anatase with a crystallite size of ~15 nm, the TiO_2 P25 consisted of 70% anatase and 30% rutile with an overall crystallite size of ~30 nm, and the TiO_2 VLP7000 consisted of 95% TiO_2 (anatase with crystallite size of ~15 nm) with sulfur and nitrogen additives. Based on the XRD analysis, the synthesized TiO_2 -s was composed of 100% anatase with a crystallite size of ~11 nm (Table 1).

The calcination of the TiO_2 HF at 550 °C did not cause the transformation of anatase to rutile and the XRD analysis of the HF-550

Table 1
Properties of the studied photocatalysts.

Sample	Pretreatment	Phase composition	Surface area, m ² /g	Pore volume, cm ³ /g	Pore size, nm
HF		anatase	327	0.35	4.3
HF-550	calcination at 550 °C		61	0.27	17.9
HF-SO ₄	H ₂ SO ₄		339	0.39	4.6
HF-1Pt	Pt deposition		300	0.36	4.8
P25		70% anatase30% rutile	81	0.27	13.4
VLP7000		anatase	296	0.41	5.6
TiO ₂ -s		anatase	222	0.14	2.4

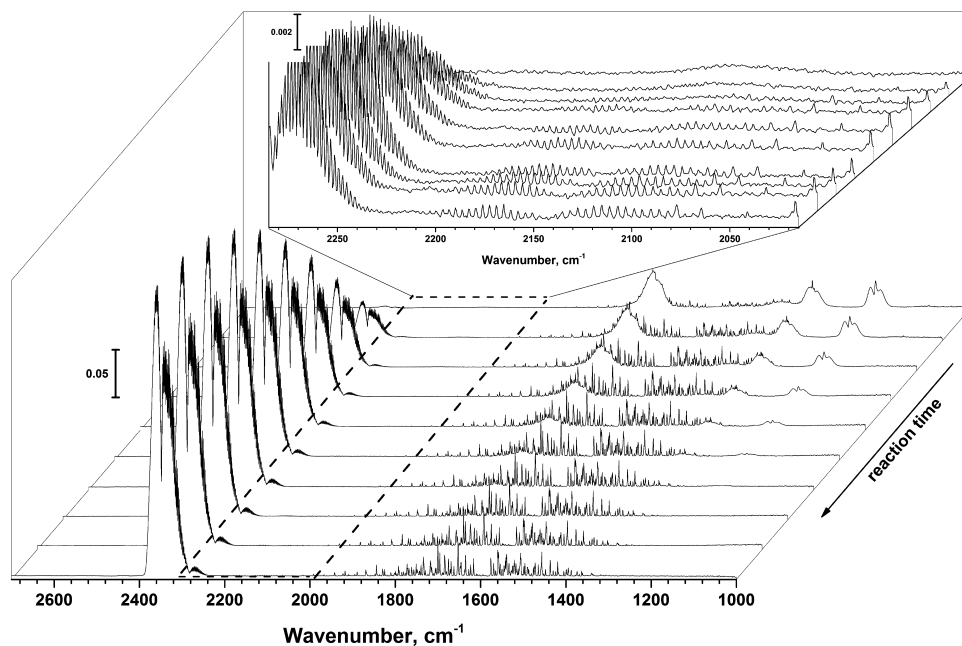


Fig. 2. Evolution of the IR spectra during acetone oxidation over $\text{TiO}_2\text{-s}$ under UV irradiation. Inset corresponds to the wavenumber range of CO absorbance.

sample exhibited 100% anatase as in the initial TiO_2 HF photocatalyst.

3.2. Kinetic experiments

3.2.1. Effect of operating parameters

Experimental conditions can substantially affect the rate and product composition of photocatalytic oxidations. Therefore, the effects of the operating parameters including the UV light intensity, initial concentration of the oxidizing substrate, relative humidity, and temperature on the formation of CO were investigated for the photocatalytic oxidation of acetone. A detailed discussion of the influence of the experimental parameters on CO formation is provided for the $\text{TiO}_2\text{-s}$ sample as an example.

Fig. 2 shows the evolution of the IR spectra during acetone oxidation over $\text{TiO}_2\text{-s}$ under UV irradiation. As the reaction time (time of UV irradiation) increased, a decrease in the intensity of the absorbance bands corresponding to acetone at 1160–1260, 1300–1500 and 1650–1850 cm^{-1} [26] was observed. This result indicates that acetone vapor was removed from the gas phase under UV irradiation. Simultaneously, an increase in the intensity of the absorbance bands corresponding to CO_2 at 2200–2400 cm^{-1} as well as the bands corresponding to H_2O at 1300–1900 cm^{-1} [27] occurred. This result indicates that under UV irradiation of $\text{TiO}_2\text{-s}$, acetone was completely oxidized to CO_2 and H_2O as the final oxidation products.

The inset in Fig. 2 shows an enlarged portion of the IR spectra at 2015–2285 cm^{-1} . A number of small narrow bands were observed at 2070–2220 cm^{-1} due to CO [27]. Therefore, CO forms during the photocatalytic oxidation of acetone over UV irradiated TiO_2 . No other gaseous products were detected.

Based on these data, the kinetic curves for acetone removal as well as CO_2 and CO accumulation were calculated using the integral form of the Beer-Lambert law and the method of spectral subtraction by minimizing the spectrum length. Typical kinetic curves of acetone, CO_2 and CO in a static reactor are shown in Fig. 3.

In this experiment, the amount of liquid acetone injected into the reactor was 1 μL , which corresponded to an acetone concentration of 1108 ppm. TiO_2 has a high adsorption capacity and

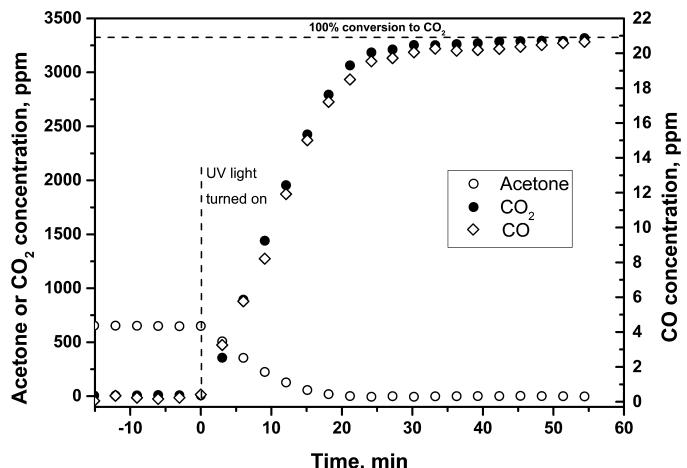


Fig. 3. Kinetic curves of acetone (○) removal as well as CO_2 (●) and CO (◊) accumulation during the photocatalytic oxidation of 1 μL acetone in a 0.3 L static reactor over $\text{TiO}_2\text{-s}$. The other experimental parameters were as follows: UV light intensity is 10.2 mW/cm^2 , initial relative humidity is 15%, and temperature is 25 $^\circ\text{C}$.

adsorption rate to acetone. Therefore, the acetone concentration that was detected after injection and adsorption-desorption equilibrium was achieved was approximately 650 ppm, which indicated that a considerable portion of the acetone was adsorbed on the photocatalyst surface. According to the stoichiometry of complete oxidation, the final concentration of CO_2 is expected 3324 ppm. The detected CO_2 concentration was approximately 3290 ppm, which corresponded to 99% conversion. The final concentration of CO was approximately 20 ppm, which corresponded to 0.6% conversion. The remaining carbon was in the form of carbonates adsorbed on the photocatalyst surface [12].

As shown in Fig. 3, the CO_2 and CO kinetic curves are similar with a curve that exhibits saturation. This result may indicate parallel pathways for CO_x formation. A previous study reported that the CO_x selectivity in the photocatalytic oxidation of hydrocarbons in a flow reactor was nearly independent of the conversion, and CO was not an intermediate to CO_2 [21].

The CO_2 and CO kinetic curves exhibited an initial linear region allowed for calculation of the initial rate of CO_2 ($W_{\text{CO}_2}^0$) and CO (W_{CO}^0) accumulation based on linear approximation. The resulting values of $W_{\text{CO}_2}^0$, W_{CO}^0 and differential selectivity of CO_2 formation (S_{CO_2}) calculated by the equation described in section 2.4 as a function of the experimental conditions are listed in Table 2.

As the UV light intensity increased from 2.6 to 10.2 mW/cm², the rate of oxidation substantially increased (i.e., increase in the rate of CO_2 accumulation). Simultaneously, the rate of CO accumulation increased. Therefore, the similar value of the differential selectivity of CO_2 formation was for both cases. For example, the selectivity was 99.49% at 2.6 mW/cm² (exp. №1), and 99.43% at 10.2 mW/cm² (exp. №3).

An increase in the initial amount of liquid acetone did not substantially affect the rate of oxidation at a low intensity (exp. №1 and №5) but led to an increase in the oxidation rate at a high intensity (exp. №3 and №6). However, in this case, the selectivities were very similar (i.e., 99.43% (exp. №3) and 99.50% (exp. №6)).

In contrast to the previous parameters, an increase in the relative humidity substantially decreased the rate of acetone oxidation. The CO_2 accumulation rate exhibited as much as a 5-fold decrease as the humidity increased from 15% to 70% (exp. №1 and №2, №3 and №4). A low oxidation rate at very high humidity level (i.e., 70%) can be explained by the formation of water film on the TiO_2 surface due to the polylayer adsorption of H_2O molecules resulting in a slow diffusion of substrate molecules to the TiO_2 surface, and blocking centers for acetone adsorption on the TiO_2 surface by H_2O molecules. As CO_2 accumulation rate, the rate of CO accumulation decreased as the relative humidity increased, and the CO_2 selectivities remained similar (i.e., 99.43% (exp. №3) and 99.38% (exp. №4)).

Table 2
Kinetic data for acetone photocatalytic oxidation over TiO_2 -s.

Exp. №	Light intensity, mW/cm ²	Initial amount of liquid acetone, μL	Relative humidity, %	$W_{\text{CO}_2}^0$, ppm/min	Err., ppm/min	W_{CO}^0 , ppm/min	Err., ppm/min	S_{CO_2} , %	Err., %
1	2.6	1	15	57	2	0.29	0.01	99.49	0.04
2			70	11.6	0.3	0.070	0.009	99.40	0.09
3	10.2		15	172	5	0.98	0.05	99.43	0.05
4			70	45	1	0.28	0.01	99.38	0.04
5	2.6	2	15	53	2	0.24	0.01	99.55	0.04
6	10.2			199	6	1.00	0.04	99.50	0.03

*The reaction temperature was 25 °C

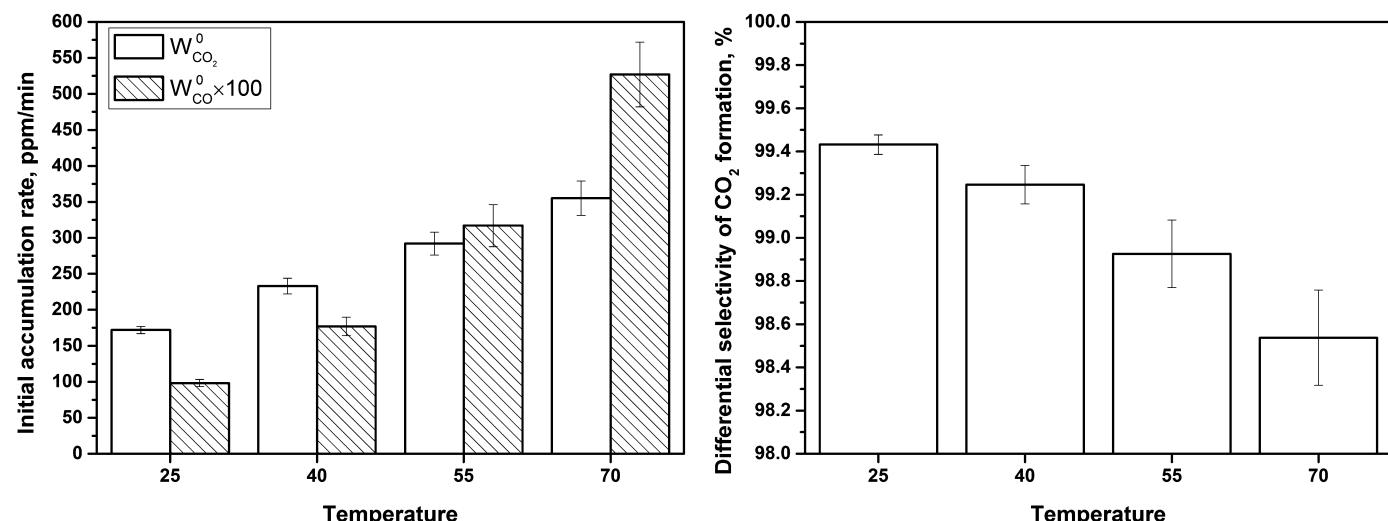


Fig. 4. Data for initial CO_2 and CO accumulation rate (left) and CO_2 selectivity (right) during acetone oxidation over TiO_2 -s at different temperatures. Experimental parameters: initial amount of liquid acetone is 1 μL , UV light intensity is 10.2 mW/cm², and relative humidity is 15%.

These results indicate that an increase in humidity does not prevent the formation of CO during the photocatalytic oxidation of acetone.

It is important to note that similar results were observed for all the photocatalysts including HF, P25 and VLP7000. The data for these experiments are provided in the SI section (Table S1).

Therefore, the operating experimental parameters including the UV light intensity, initial concentration of the oxidizing substrate and relative humidity had not significant effect on the differential CO_2 selectivity. When the rate of CO_2 formation increased (decreased) due to a change in the parameters, the rate of CO formation also proportionally increased (decreased), and the selectivity was similar.

The opposite effect was observed with increasing the reaction temperature. The results of the kinetic experiments with various temperatures are shown in Fig. 4. The rates of CO_2 and CO accumulation increased as the reactor temperature increased from 25 to 70 °C. But in contrary to the cases described above, the increase in the CO rate was higher than the increase in the CO_2 rate that resulted in monotonic decrease in the CO_2 selectivity from 99.4% at 25 °C to 98.5% at 70 °C. It is important to note that similar results were also observed for the TiO_2 HF photocatalyst (Fig. S1 in the SI section).

Therefore, an increase in the reaction temperature resulted in an increase in the photooxidation rate and a decrease in the CO_2/CO selectivity.

3.2.2. Effect of the photocatalyst

Next, we compared the oxidation of acetone vapor over all the photocatalysts.

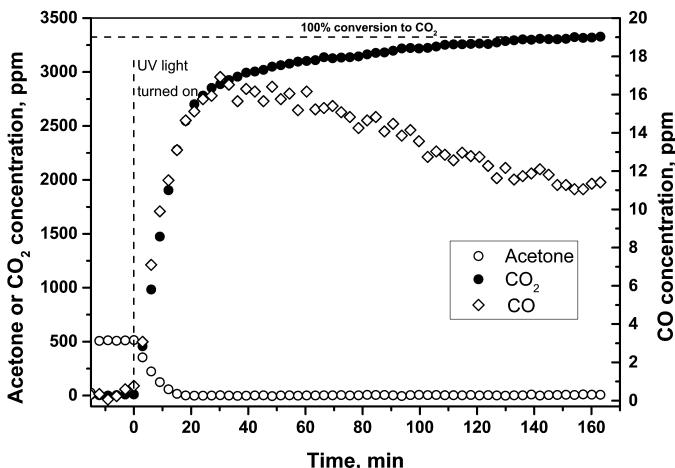


Fig. 5. Kinetic curves of acetone (○), CO₂ (●) and CO (◊) during the photocatalytic oxidation of 1 μL acetone in a 0.3 L static reactor over HF. The other experimental parameters were as follows: UV light intensity is 10.2 mW/cm², initial relative humidity is 15%, and temperature is 25 °C.

In contrast to the synthesized TiO₂-s sample, the commercially available photocatalysts (i.e., HF, P25 and VLP7000) demonstrated low activity for the photocatalytic oxidation of CO under UV irradiation. As shown in Fig. 5, after reaching a maximum value, the CO concentration began to decrease gradually, which indicates that CO undergoes photocatalytic oxidation on the TiO₂ surface during long-term UV irradiation. For example, for the HF photocatalyst, the initial rate of CO accumulation was 0.81 ppm/min, and the rate of CO removal was 0.04 ppm/min. The highest CO removal rate was observed for the VLP7000 photocatalyst. However, this rate was 17 times lower than the rate of CO accumulation. Therefore, the rate of CO oxidation is much lower than the rate of its formation, and this value can be neglected in the calculation of the CO accumulation rate.

All the photocatalysts were compared using the same experimental conditions. Consistent with the results for TiO₂-s, only CO₂, H₂O and CO were detected as final oxidation products for all the commercial photocatalysts. Fig. 6 shows the results of the kinetic experiments for acetone oxidation over all the photocatalysts (i.e., HF, P25, VPL7000 and TiO₂-s). Because the photocatalysts were synthesized using different methods, they demonstrated different

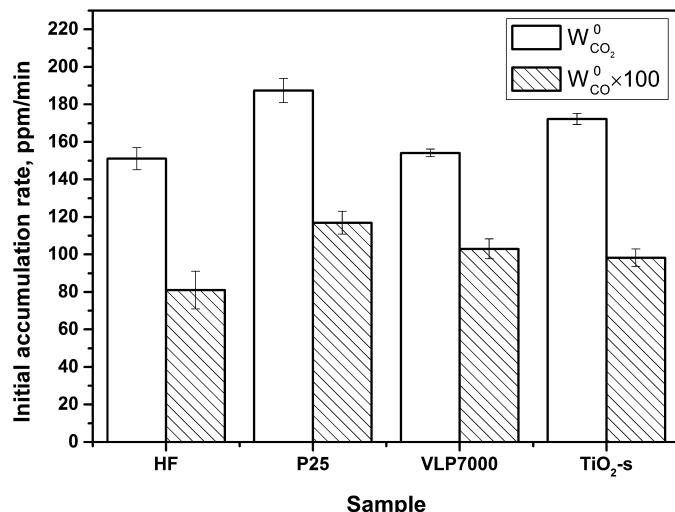


Fig. 6. Data for initial CO₂ and CO accumulation rate (left) and CO₂ selectivity (right) during acetone oxidation over several photocatalysts. Experimental parameters: initial amount of liquid acetone is 1 μL, UV light intensity is 10.2 mW/cm², relative humidity is 15%, and temperature is 25 °C.

activities for the oxidation of acetone. The rate of CO₂ accumulation increased in the following sequence: HF ≈ VLP7000 < TiO₂-s < P25. At the same time, the selectivity of CO₂ formation towards CO formation was very similar and ranged from 99.34% for VLP7000 to 99.47% for HF. Therefore, taking into account the experimental error, all the photocatalysts exhibited similar selectivities. This result indicates that the formation of CO was not determined by the primary processes occurring in the TiO₂ particle but by the subsequent redox surface reactions because the crystal phase composition and crystallite size, which are different for all the photocatalysts, did not influence the CO₂/CO selectivity.

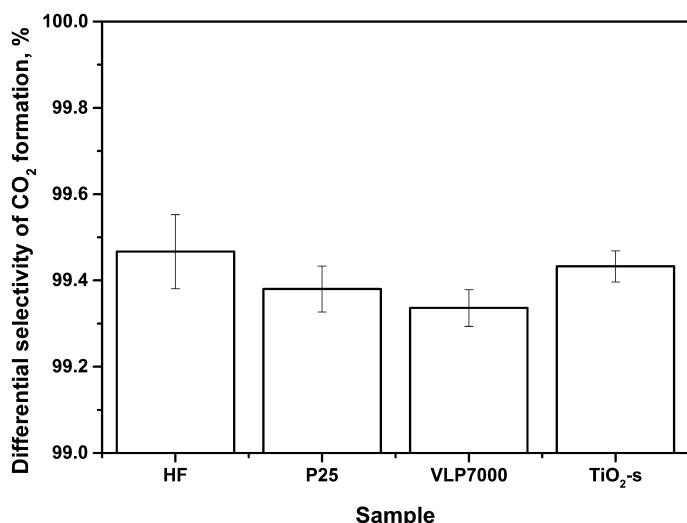
Based on these data, the formation of CO always occurs during the photocatalytic oxidation of acetone on the TiO₂ surface.

3.2.3. Effect of the photocatalyst pretreatment

Several treatments can be used to modify a TiO₂ photocatalyst and alter its photocatalytic activity. In our study, TiO₂ was treated using sulfuric acid, calcination and noble metal deposition. Sulfation can increase the TiO₂ surface acidity and result in the formation of an amorphous layer on the surface [28]. During calcination, textural characteristics, surface composition and the number of hydroxyl groups can change [29]. Deposition of Pt can alter the electronic properties of the photocatalyst as well as its CO adsorption characteristics [30].

In this section, the influence of these treatments on the formation of CO during the oxidation of acetone will be discussed. The TiO₂ HF photocatalyst was modified to obtain sulfated (HF-SO₄), calcined (HF-550) and 1 wt.% Pt- (HF-1Pt) or 0.02 wt.% Pt-loaded (HF-0.02Pt) samples.

The results of these experiments are shown in Fig. 7. The treatment of TiO₂ by sulfuric acid or its calcination led to a substantial increase in the acetone oxidation rate. The HF-SO₄ sample exhibited a CO₂ rate of 218 ppm/min, which was much higher than that for the initial HF photocatalyst (i.e., 151 ppm/min). The highest CO₂ rate was observed for the HF-550 sample (i.e., 250 ppm/min) despite a substantial decrease in the specific surface area due to calcination (see Table 1). In addition to an increase of CO₂ formation rate, the treatments of HF increased the rate of CO formation. The CO formation rates were 0.81, 1.28 and 1.48 ppm/min for HF, HF-SO₄ and HF-550, respectively. As a result, the CO₂ selectivity shown in Fig. 7 was nearly the same value for all the cases (i.e., 99.47% for HF, 99.42% for HF-SO₄ and 99.41% for HF-550). This result indicates that changes in the surface composition due to sulfation and cal-



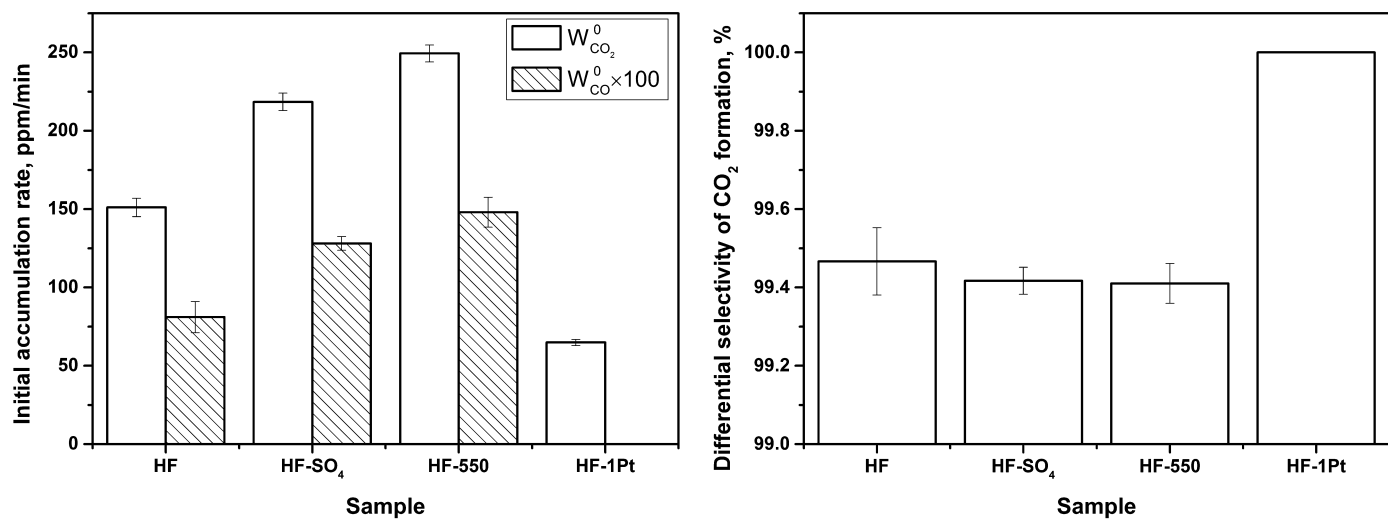


Fig. 7. Data for initial CO₂ and CO accumulation rate (left) and CO₂ selectivity (right) during acetone oxidation over initial and pretreated HF. Experimental parameters: initial amount of liquid acetone is 1 μ L, UV light intensity is 10.2 mW/cm², relative humidity is 15%, and temperature is 25 °C.

cination did not influence the selectivity of CO₂ formation relative to CO formation. Therefore, CO formation was not determined by the formation of active surface species but by the transformation pathways of the oxidizing substrate.

The only way to completely prevent the formation of CO was the deposition of 1 wt.% platinum on the titanium dioxide. In this case, CO was not detected in the gas phase during the oxidation of 1 or 2 μ L of acetone at low or high UV intensity.

This result can be explained by two factors as follows: First, platinum changes the reaction pathways of the surface reactions and inhibits the reactions involved in CO formation by catalyzing the reactions of direct oxidation to CO₂.

Second, the presence of platinum on the TiO₂ surface increases the rate of CO oxidation. The oxidation of CO over Pt/TiO₂ can occur via a thermal oxidation pathway [31] as well as a photocatalytic oxidation pathway when UV irradiation results in acceleration of the oxidation rate [32]. Therefore, even if CO is formed on the surface of the platinized photocatalyst during the acetone oxidation, it is rapidly oxidized to CO₂ before it can leave surface and enter the gas phase. Therefore, no CO was detected in the gas phase.

To evaluate a key factor in the prevention of CO accumulation in the case of the Pt-loaded catalysts, the experiment with the photocatalyst containing a smaller amount of platinum was performed. Fig. 8 shows the CO₂ and CO kinetic curves during the oxidation of 1 μ L of acetone over 0.02 wt.% Pt-loaded sample. For the HF-0.02Pt sample, CO was detected in the gas phase, and after reaching a maximum value, its concentration began to decrease gradually. The initial rate of CO accumulation was 0.86 ppm/min, and the rate of CO removal was 0.11 ppm/min. This result indicates that CO does really form during the photooxidation over Pt/TiO₂. In contrast to the HF-1Pt sample, a low amount of Pt cannot prevent the formation of CO and lead to its oxidation to CO₂ only during long-term UV irradiation. Therefore, the second factor is more feasible for Pt/TiO₂.

The main disadvantage of TiO₂ modification by Pt is that the activity of the platinized photocatalyst depends on the method of platinum deposition. In our case, a substantial decrease in the rate of acetone oxidation was observed for 1 wt.% Pt-loaded photocatalyst. For example, the initial rate of CO₂ accumulation was 151 ppm/min for HF and 65 ppm/min for HF-1Pt.

Therefore, modification of the TiO₂ surface with platinum had a significant influence on the CO₂ selectivity. Based on other our studies, other noble metals, such as Pd, Au etc., can also be employed

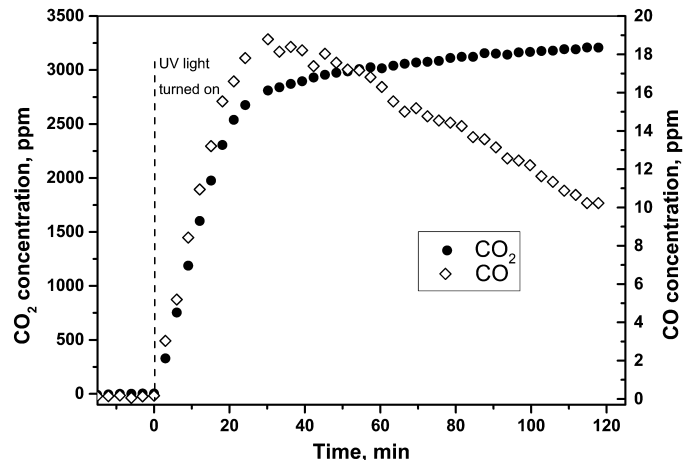


Fig. 8. Kinetic curves of CO₂ (●) and CO (◊) during the photocatalytic oxidation of 1 μ L acetone in a 0.3 L static reactor over HF-0.02Pt. The other experimental parameters were as follows: UV light intensity is 10.2 mW/cm², initial relative humidity is 15%, and temperature is 25 °C.

for TiO₂ modification to prevent CO evolution during the photooxidation process.

3.2.4. Effect of type of oxidizing substrate

To determine the formation of CO is specific for the photocatalytic oxidation of acetone or is observed during the oxidation of other VOCs, we tested other organic substrates. Three groups of organic compounds were chosen as follows: a homologous series of C₁–C₄ alcohols and a homologous series of C₆–C₁₀ alkanes to investigate the effect of the number of C atoms in the substrate molecule on CO formation as well as C₆ hydrocarbons from hexane to benzene to investigate the influence of the unsaturation degree on CO formation.

3.2.4.1. Homologous series of alcohols. Fig. 9 shows the kinetic data for the photocatalytic oxidation of C₁–C₄ alcohols over the HF photocatalyst. The results for methanol differ from those of the other alcohols. Along with a high rate of CO₂ accumulation during the oxidation of methanol, a high rate of CO accumulation was observed. In this case, the CO₂ selectivity was the lowest (i.e., 99.17%). The final concentration of CO during the photocatalytic oxidation of

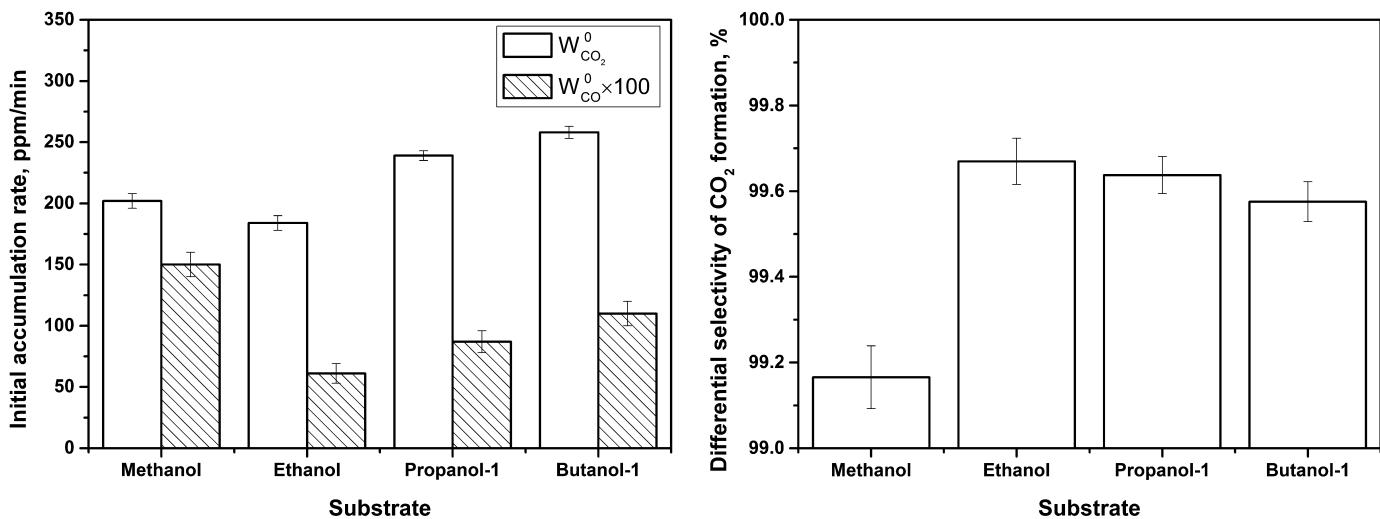


Fig. 9. Data for initial CO_2 and CO accumulation rate (left) and CO_2 selectivity (right) during alcohol oxidation over HF. Experimental parameters: initial amount of liquid substrate is 1 μ L, UV light intensity is 10.2 mW/cm 2 , relative humidity is 15%, and temperature is 25 °C.

methanol was approximately 15 ppm, which corresponds to a conversion of 0.73%. During the oxidation of the other alcohols, the CO_2 rate was either lower (ethanol) or higher (propanol or butanol) than that for the oxidation of methanol. However, in all the cases, the CO rate was much lower. Therefore, the CO_2 selectivity was higher compared to that for methanol vapor oxidation (i.e., from 99.67% for ethanol to 99.58% for butanol). The CO_2 selectivity for the oxidation of C₂–C₄ alcohols was similar to the selectivity for the acetone oxidation (see Fig. 6).

Among these substrates, only methanol, which contains one C atom, exhibited the lowest CO_2 selectivity. The difference between the oxidation of methanol and the oxidation of the other alcohols indicates that during the gradual oxidation of organic compounds, the largest effect was observed for the oxidation of the last C atom in the molecule.

3.2.4.2. Homologous series of alkanes. Fig. 10 shows the kinetic data obtained during the oxidation of *n*-hydrocarbons with different numbers of C atoms. The CO_2 rate slightly decreased for the sequence from hexane to decane because an increase in the size of the substrate results in fewer places being available for its adsorption. Therefore, lower photooxidation rate was observed.

Similar to alcohol photocatalytic oxidation, the CO_2 selectivity during the oxidation of hydrocarbons slightly decreased as the number of C atoms in the oxidizing substrate increased (i.e., from 98.91% for *n*-hexane to 98.66% for *n*-decane) but not significantly. Based on comparison to the results shown in Fig. 9, the CO_2 selectivity for the oxidation of *n*-hydrocarbons was slightly lower than that for the oxidation of alcohols.

Based on the results for the oxidation of alcohols and alkanes, the number of C atoms in the oxidizing substrate is not a key factor that affects the formation of CO .

3.2.4.3. C₆ hydrocarbons with various unsaturation degrees. The strongest effect of the oxidizing substrate was observed during the photocatalytic oxidation of the C₆ hydrocarbons. The results of these experiments are shown in Fig. 11. The CO_2 accumulation rates during the oxidation of hexane and cyclohexane were similar (i.e., 124 and 136 ppm/min, respectively). A further increase in unsaturation resulted in a substantial decrease in the CO_2 rate (i.e., 68 ppm/min for cyclohexene and 14 ppm/min for benzene), which indicates a strong loss of photocatalytic activity during the oxidation of aromatic compounds compared to that during the oxi-

dation of saturated hydrocarbons. In contrast to results for other VOCs (i.e., acetone, alcohols and alkanes), the CO rate did not decrease proportionally to the CO_2 rate. As a result, the CO_2 selectivity substantially decreased as the unsaturation degree of the C₆ hydrocarbons increased. For example, the selectivity was 98.91% for hexane, 96.6% for cyclohexene and 93.3% for benzene. The conversion of benzene to CO was approximately 5%, which is the highest value among all the studied substrates. This result indicates the strong influence of the type of oxidizing substrate on the CO formation.

Einaga et al. [21] observed the formation of carbon deposits on the TiO₂ surface during the oxidation of several hydrocarbons using UV-vis and FTIR spectroscopy. A higher amount of deposits was observed for aromatic compounds (benzene and toluene) compared to that observed for cyclohexene. The formation of polycarbon structures that are difficult to oxidize completely to CO_2 may explain the formation of a high amount of CO during the photooxidation of benzene.

3.2.5. Mechanism of CO formation

One can assume that the formation of CO occurs via the detachment of an O atom from the CO_2 molecule (its reduction) due to interaction with O vacancies formed on TiO₂ surface during the photocatalytic oxidation of organic substrates. These processes have been described in studies related to CO_2 photoreduction. However, in our case, this mechanism for CO formation appears to be unlikely for the following reasons:

- (1) In general, photoreduction of CO_2 occurs in an oxygen-free atmosphere where only the CO_2 molecule can act as an oxidant [33].
- (2) The rate of this process is slow. The typical value of CO formation is approximately several $\mu\text{mol g}^{-1} \text{h}^{-1}$ [34].

Therefore, during the photocatalytic oxidation of organic compounds in air in the presence of a large amount of oxygen (and water), the contribution from this process should be negligible.

Carbon monoxide is most likely formed during certain steps in the oxidation of the organic substrate.

The common pathway for photocatalytic oxidation involves organic substrate coming into contact with an irradiated TiO₂ surface being activated by active species (i.e., charge carriers or oxidants, such as hydroxyl radicals) and converted to a radical inter-

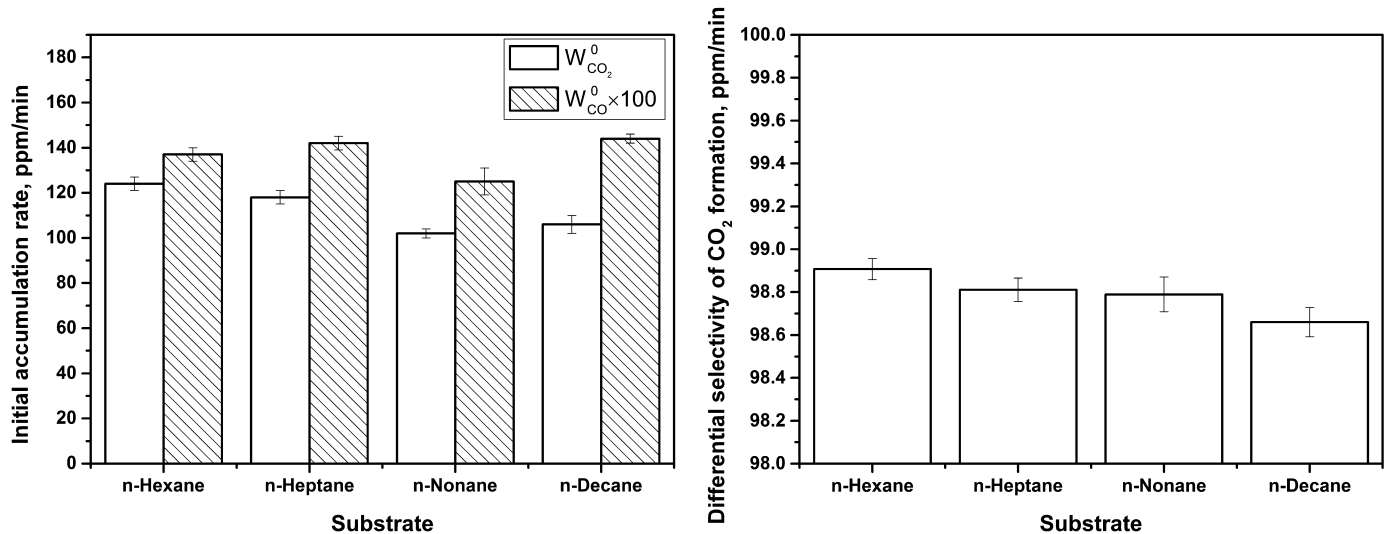


Fig. 10. Data for initial CO_2 and CO accumulation rate (left) and CO_2 selectivity (right) during *n*-hydrocarbon oxidation over HF. Experimental parameters: initial amount of liquid substrate is 1 μL , UV light intensity is 10.2 mW/cm^2 , relative humidity is 15%, and temperature is 25 $^\circ\text{C}$.

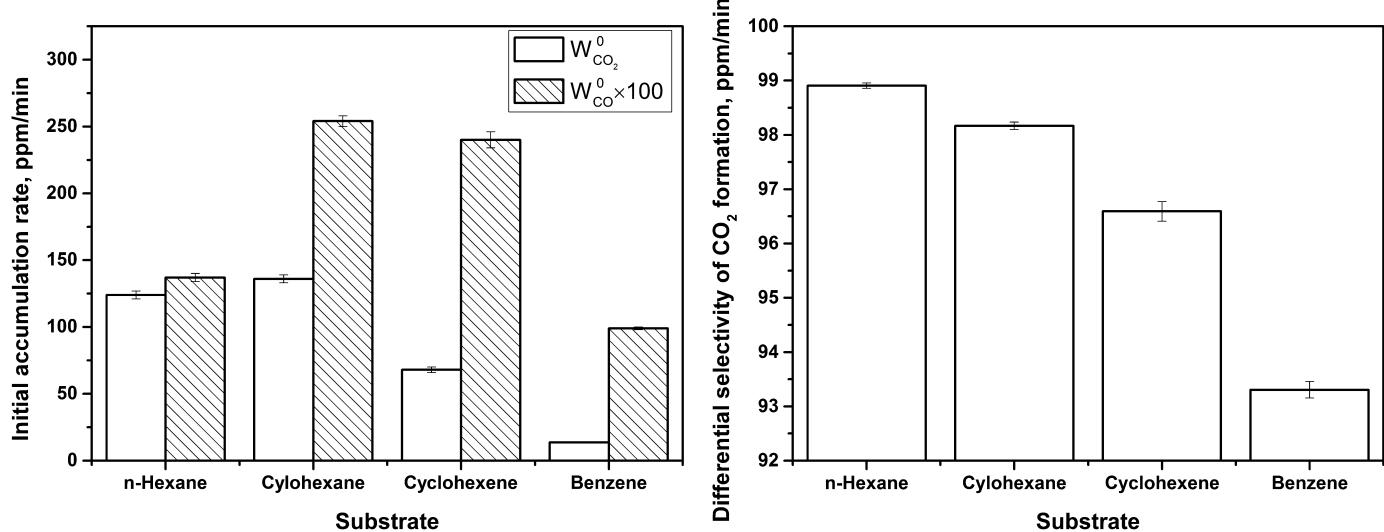


Fig. 11. Data for initial CO_2 and CO accumulation rate (left) and selectivity of CO_2 formation (right) during C_6 hydrocarbon oxidation over HF. Experimental parameters: initial amount of liquid substrate is 1 μL , UV light intensity is 10.2 mW/cm^2 , relative humidity is 15%, and temperature is 25 $^\circ\text{C}$.

mediate. Due to key sequential transformations, this intermediate is converted to a new organic molecule (or molecules) with a fewer number of C atoms. The remaining carbon is released into the gas phase in the form of CO_2 . The resulting organic molecule undergoes further transformations that ultimately result in complete mineralization of the starting substrate.

These surface intermediates can be decomposed to form CO_2 and CO as products. For example, in the sequential oxidation of an organic substrate, one of the last intermediates may be formic acid or the formate anion [35]. We observed the formation of formic acid even in the gas phase during the oxidation of diethyl sulfide vapor [17]. In the presence of dehydrating compounds (e.g., sulfuric or phosphoric acids), formic acid has well known to decompose into CO and water as follows:

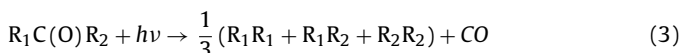


The rate of this process increases as the temperature increases. Therefore, due to the presence of various factors, such as UV light and local heating the photocatalyst due to light absorbance and

the recombination of the charge carriers, partial decomposition of formic acid or formates to CO may occur on the irradiated TiO_2 surface, which may explain the much lower CO_2 selectivity during the oxidation of methanol, which contains only one C atom, compared to that during the oxidation of other alcohols, such as ethanol, propanol and butanol (Fig. 9). This suggestion is also supported by the fact that the CO_2 selectivity decreased as the reaction temperature increased (Fig. 4).

CO can also form from the decomposition of other organic surface intermediates. As was shown in section 1, aldehydes and ketones are often the intermediates during the photocatalytic oxidation of VOCs. In this case, an important role can be the decomposition of aldehyde (or ketone) intermediates forming on the irradiated TiO_2 surface.

Aldehydes and ketones absorbs UV light with wavelengths from 200 to 350 nm due to the presence of $\text{C}=\text{O}$ group in these molecules. Absorption of UV light in this range has well known to result in the photochemical decomposition of these substrates with the formation of CO as follows [36]:



In addition to the photochemical decomposition, the photocatalytic decomposition of aldehydes (or ketones) can occur similarly.

In contrast to aldehydes and ketones, the photochemical decomposition of carboxylic acids results in the formation of CO_2 as a product. Therefore, the decomposition of aldehyde (or ketone) intermediates forming on the surface of irradiated photocatalyst may be a key step responsible for CO formation during the photocatalytic oxidation of non-aromatic VOCs.

Finally, as was mentioned in section 3.2.4.3, the formation of high amount of CO during the photocatalytic oxidation of aromatic compounds may be related to the formation of polycarbon structures that are difficult to oxidize completely to CO_2 .

From a practical point of view, for the oxidation of substances with a concentration less than 10 ppm, the formation of carbon monoxide will not play a significant role because its quantity will be very small (ppb level). However, with regards to the oxidation of more concentrated mixtures (100–1000 ppm) or aromatic mixtures, this problem is more important. From a scientific point of view, further research is required to elucidate the mechanism of CO formation during the photocatalytic oxidation of VOCs.

4. Conclusions

Three commercially available TiO_2 photocatalysts and one synthesized TiO_2 catalyst were employed to investigate the oxidation of VOCs including acetone, alcohols and hydrocarbons with a focus on the formation of CO as a by-product. The following conclusions can be made:

- (1) The formation of CO always occurs in the photocatalytic oxidation of acetone on the TiO_2 surface. In general, the acetone conversion to CO was less than 1%. The experimental parameters including light intensity, initial substrate concentration and humidity as well as the photocatalyst and its pretreatment by sulfation or calcination did not have a significant effect on the differential selectivity of CO_2 formation towards CO formation. The average CO_2 selectivity for acetone oxidation (for 27 experiments with different conditions and samples) was $99.48 \pm 0.04\%$. On the other hand, an increase in the reaction temperature resulted in an increase in the photooxidation rate and a decrease in the CO_2 selectivity.
- (2) The deposition of a noble metal (i.e., Pt) on the surface of TiO_2 prevents the formation of CO during the photocatalytic oxidation of acetone. For the 1 wt.% Pt-loaded photocatalyst, CO was not detected in the gas phase during the photocatalytic oxidation of acetone at low and high UV intensities.
- (3) The formation of CO was also observed during the photocatalytic oxidation of other VOCs (i.e., alcohols and hydrocarbons). The type of oxidizing substrate (i.e., alcohol, ketone, alkane, and aromatic) has a strong influence on CO formation. The increase in the number of carbon atoms in the C_2 – C_4 alcohols and C_6 – C_{10} n-hydrocarbons homologous series slightly decreased the CO_2 selectivity. The largest effect was related to the unsaturation degree of the C_6 hydrocarbons. The CO_2 selectivity decreased from 98.9% for hexane to 93.3% for benzene. Benzene had the highest conversion to CO (approximately 5%) among all the studied substrates.

Acknowledgements

This work was supported by the Skolkovo Foundation (Grant Agreement for Russian educational organizations no. 5 of

30.12.2015) and the Russian Fund for Basic Research (project 16-33-00823 мол_а).

Appendix A. Supplementary data

Supplementary data associated with this article can be found, in the online version, at <http://dx.doi.org/10.1016/j.apcatb.2016.07.044>.

References

- [1] Environmental Protection in Russia (Statistics Book), Federal State Statistics Service (Rosstat), Moscow, 2014.
- [2] L. Kavan, M. Gratzel, S.E. Gilbert, C. Klemenz, H.J. Scheel, Electrochemical and photoelectrochemical investigation of single-crystal anatase, *J. Am. Chem. Soc.* 118 (1996) 6716–6723.
- [3] A. Fujishima, X.T. Zhang, D.A. Tryk, TiO_2 photocatalysis and related surface phenomena, *Surf. Sci. Rep.* 63 (2008) 515–582.
- [4] N. Serpone, Brief introductory-remarks on heterogeneous photocatalysis, *Sol. Energy Mater. Sol. Cell* 38 (1995) 369–379.
- [5] O. Carp, C.L. Huisman, A. Reller, Photoinduced reactivity of titanium dioxide, *Prog. Solid State Chem.* 32 (2004) 33–177.
- [6] K. Wada, K. Yoshida, T. Takatani, Y. Watanabe, Selective photooxidation of light alkanes using solid metal-oxide semiconductors, *Appl. Catal. A: Gen.* 99 (1993) 21–36.
- [7] X. Deng, Y. Yue, Z. Gao, Gas-phase photo-oxidation of organic compounds over nanosized TiO_2 photocatalysts by various preparations, *Appl. Catal. B: Environ.* 39 (2002) 135–147.
- [8] C. Wu, Y. Yue, X. Deng, W. Hua, Z. Gao, Investigation on the synergistic effect between anatase and rutile nanoparticles in gas-phase photocatalytic oxidations, *Catal. Today* 93–95 (2004) 863–869.
- [9] D.S. Muggli, J.T. McCue, J.L. Falconer, Mechanism of the photocatalytic oxidation of ethanol on TiO_2 , *J. Catal.* 173 (1998) 470–483.
- [10] A.V. Vorontsov, V.P. Dubovitskaya, Selectivity of photocatalytic oxidation of gaseous ethanol over pure and modified TiO_2 , *J. Catal.* 221 (2004) 102–109.
- [11] D.S. Muggli, J.L. Falconer, Catalyst design to change selectivity of photocatalytic oxidation, *J. Catal.* 175 (1998) 213–219.
- [12] D.V. Kozlov, A.V. Vorontsov, P.G. Smirniotis, E.N. Savinov, Gas-phase photocatalytic oxidation of diethyl sulfide over TiO_2 : kinetic investigations and catalyst deactivation, *Appl. Catal. B: Environ.* 42 (2003) 77–87.
- [13] E. Piera, J.A. Ayllon, X. Domenech, J. Peral, TiO_2 deactivation during gas-phase photocatalytic oxidation of ethanol, *Catal. Today* 76 (2002) 259–270.
- [14] M. Takeuchi, J. Deguchi, S. Sakai, M. Anpo, Effect of H_2O vapor addition on the photocatalytic oxidation of ethanol, acetaldehyde and acetic acid in the gas phase on TiO_2 semiconductor powders, *Appl. Catal. B: Environ.* 96 (2010) 218–223.
- [15] W. Wang, Y. Ku, Photocatalytic degradation of gaseous benzene in air streams by using an optical fiber photoreactor, *J. Photochem. Photobiol. A: Chem.* 159 (2003) 47–59.
- [16] D.S. Selishchev, P.A. Kolinko, D.V. Kozlov, Influence of adsorption on the photocatalytic properties of TiO_2 /AC composite materials in the acetone and cyclohexane vapor photooxidation reactions, *J. Photochem. Photobiol. A: Chem.* 229 (2012) 11–19.
- [17] D. Selishchev, D. Kozlov, Photocatalytic oxidation of diethyl sulfide vapor over TiO_2 -based composite photocatalysts, *Molecules* 19 (2014) 21424–21441.
- [18] D.S. Selishchev, I.P. Karaseva, V.V. Uvaev, D.V. Kozlov, V.N. Parmon, Effect of preparation method of functionalized textile materials on their photocatalytic activity and stability under UV irradiation, *Chem. Eng. J.* 224 (2013) 114–120.
- [19] A.V. Vorontsov, E.N. Savinov, E.N. Kurkin, O.D. Torbova, V.N. Parmon, Kinetic features of the steady state photocatalytic CO oxidation by air on TiO_2 , *React. Kinet. Catal. Lett.* 62 (1997) 83–88.
- [20] D.S. Muggli, L.F. Ding, Photocatalytic performance of sulfated TiO_2 and Degussa P-25 TiO_2 during oxidation of organics, *Appl. Catal. B: Environ.* 32 (2001) 181–194.
- [21] H. Einaga, S. Futamura, T. Ibusuki, Heterogeneous photocatalytic oxidation of benzene, toluene, cyclohexene and cyclohexane in humidified air: comparison of decomposition behavior on photoirradiated TiO_2 catalyst, *Appl. Catal. B: Environ.* 38 (2002) 215–225.
- [22] F. Thevenet, O. Guaitella, J.M. Herrmann, A. Rousseau, C. Guillard, Photocatalytic degradation of acetylene over various titanium dioxide-based photocatalysts, *Appl. Catal. B: Environ.* 61 (2005) 58–68.
- [23] J. Jeong, K. Sekiguchi, W. Lee, K. Sakamoto, Photodegradation of gaseous volatile organic compounds (VOCs) using TiO_2 photoirradiated by an ozone-producing UV lamp: decomposition characteristics identification of by-products and water-soluble organic intermediates, *J. Photochem. Photobiol. A: Chem.* 169 (2005) 279–287.
- [24] A. Banisharif, A.A. Khodadadi, Y. Mortazavi, A. Anarak Firooz, J. Beheshtian, S. Agah, S. Menbari, Highly active Fe_2O_3 -doped TiO_2 photocatalyst for degradation of trichloroethylene in air under UV and visible light irradiation: experimental and computational studies, *Appl. Catal. B: Environ.* 165 (2015) 209–221.

[25] D. Kozlov, A. Besov, Method of spectral subtraction of gas-phase fourier transform infrared (FT-IR) spectra by minimizing the spectrum length, *Appl. Spectrosc.* 65 (2011) 918–923.

[26] NIST Standart Reference Database 79 Quantitative Infrared of Database 1998.

[27] K. Nakamoto, Infrared and Raman Spectra of Inorganic and Coordination Compounds, Part A, Theory and Applications in Inorganic Chemistry, 6th ed., John Wiley & Sons, New Jersey, 2009.

[28] D.V. Kozlov, A.V. Vorontsov, Sulphuric acid and Pt treatment of the photocatalytically active titanium dioxide, *J. Catal.* 258 (2008) 87–94.

[29] Q. Zhang, L. Gao, J. Guo, Effects of calcination on the photocatalytic properties of nanosized TiO₂ powders prepared by TiCl₄ hydrolysis, *Appl. Catal. B: Environ.* 26 (2000) 207–215.

[30] A.V. Vorontsov, I.V. Stoyanova, D.V. Kozlov, V.I. Simagina, E.N. Savinov, Kinetics of the photocatalytic oxidation of gaseous acetone over platinized titanium dioxide, *J. Catal.* 189 (2000) 360–369.

[31] N. Li, Q.-Y. Chen, L.-F. Luo, W.-X. Huang, M.-F. Luo, G.-S. Hu, J.-Q. Lu, Kinetic study and the effect of particle size on low temperature CO oxidation over Pt/TiO₂ catalysts, *Appl. Catal. B: Environ.* 142–143 (2013) 523–532.

[32] S. Hwang, M.C. Lee, W. Choi, Highly enhanced photocatalytic oxidation of CO on titania deposited with Pt nanoparticles: kinetics and mechanism, *Appl. Catal. B: Environ.* 46 (2003) 49–63.

[33] C.-C. Yang, Y.-H. Yu, B. van der Linden, J.C.S. Wu, G. Mul, Artificial photosynthesis over crystalline TiO₂-based catalysts: fact or fiction? *J. Am. Chem. Soc.* 132 (2010) 8398–8406.

[34] B. Fang, A. Bonakdarpour, K. Reilly, Y. Xing, F. Taghipour, D.P. Wilkinson, Large-scale synthesis of TiO₂ microspheres with hierarchical nanostructure for highly efficient photodriven reduction of CO₂ to CH₄, *ACS Appl. Mater. Interfaces* 6 (2014) 15488–15498.

[35] C.H. Ao, S.C. Lee, J.Z. Yu, J.H. Xu, Photodegradation of formaldehyde by photocatalyst TiO₂: effects on the presences of NO, SO₂ and VOCs, *Appl. Catal. B: Environ.* 54 (2004) 41–50.

[36] F.W. Kirkbride, R.G.W. Norrish, Photochemical properties of the carbonyl group, *Trans. Faraday Soc.* 27 (1931) 404–409.